

curves are shown in Figure 11 (differential pulse,²⁰ differential normal pulse,^{12,26} differenced normal pulse,³⁰ staircase,³¹ and square wave voltammetry) and in Figure 12 (normal¹¹ and reverse^{32,33} pulse voltammetry). The values of $E_{1/2}^r$, α , and $\log \kappa\tau^{1/2}$, displayed in Table III, all fall within the calculated confidence intervals. With the possible exception of reverse pulse voltammetry the quality of the fit is about the same in each case. Note the greater sensitivity of the voltammetric wave (Figure 11), and, among the differential or derivative techniques (Figure 10), the greater sensitivity of square wave voltammetry. Of these techniques only normal and, of course, differenced normal pulse voltammetry have well-established, although questionable, methods of data analysis, as described above. In the limit of small step height and high frequency, staircase voltammetry approaches linear scan voltammetry, and so these voltammograms could, with some resulting errors, be analyzed as such. The data analysis employed here depends on the calculation of currents over time intervals short compared with the pulse time, but the calculations must be done over the entire electrolysis time. Of these techniques reverse pulse and differential pulse voltammetry are the only ones with extended electrolysis times. In reverse pulse, only one such calculation needs to be performed, but for differential pulse the calculation must be done for each experimental point. With our system as described the entire curve-fitting procedure typically takes minutes for square wave, tens of minutes for reverse pulse, and hours for differential pulse voltammetry. Thus, the latter is not competitive as a technique

for kinetic investigations. More detailed consideration of techniques other than square wave voltammetry is beyond the scope of this work. The response in differenced normal, differential normal, and differential pulse voltammetry for quasi-reversible systems is discussed in detail by Lovrić et al.³⁴

We conclude from this work that square wave voltammetry is an excellent technique for determining kinetic parameters. Its inherent reliance on computer-based systems for variation of experimental parameters and for numerical calculation of the response expected from various models may be turned to advantage by using objective techniques for curve fitting which yield best values of the parameters of the model along with realistic estimates of their confidence intervals. The techniques used here also apply without modification to all pulse voltammetric wave forms. As in other cases, the modified simplex algorithm must be used with judgment, for the optimum values found may represent saddle points or local maxima. The confidence intervals lack rigorous statistical definition but are well-defined mathematically and seem to provide realistic estimates of the uncertainty in the values of the derived parameters.

Acknowledgment. This material was presented in part at the Middle Atlantic Regional American Chemical Society Meeting, Newark, DE, April 21-24, 1982. This work was supported in part by the National Science Foundation under Grants CHE 7917543 and CHE 8305748.

Registry No. Zn, 7440-66-6; NaNO₃, 7631-99-4.

(30) Anderson, J. E.; Bond, A. M. *Anal. Chem.* 1981, 53, 504-8.

(31) Christie, J. H.; Lingane, P. J. *J. Electroanal. Chem.* 1965, 10, 176-82.

(32) Osteryoung, Janet; Kirowa-Eisner, Emilia. *Anal. Chem.* 1980, 52, 62-6.

(33) Oldham, K. B.; Parry, E. P. *Anal. Chem.* 1970, 42, 229-33.

(34) Lovrić, Milivoj; O'Dea, J. J.; Osteryoung, Janet. *Anal. Chem.* 1983, 55, 704-8.

(35) Baranski, A.; Fitale, S.; Galus, Z. *J. Electroanal. Chem.* 1975, 60, 175-81.

(36) Dillard, J. W.; O'Dea, J. J.; Osteryoung, R. A. *Anal. Chem.* 1979, 51, 115-9.

Thermal-Induced and Photoinduced Atropisomerization of Picket-Fence Porphyrins, Metalloporphyrins, and Diacids: A Means for Examining Porphyrin Solution Properties

Ruth A. Freitag and David G. Whitten*

Department of Chemistry, University of North Carolina, Chapel Hill, North Carolina 27514 (Received: January 3, 1983)

An investigation of the thermal-induced and photoinduced atropisomerization of the free base, diacid, and metal complexes of tetrakis(*o*-pivalamidophenyl)porphyrin (H₂PF, TPiv), tetrakis(*o*-hexadecanamidophenyl)porphyrin (H₂PF, THA), and tetrakis(*o*-propionamidophenyl)porphyrin (H₂PF, TPro) was carried out. The isomerization process involves rotation of a single phenyl ring through a coplanar transition state, which requires substantial distortion from planarity of the porphyrin core. Relative thermal isomerization rates and photoisomerization efficiencies were found to depend on the size of the ortho substituent as well as on the atom(s) coordinated to the central core. The nature of the latter dependence suggests that porphyrin deformability in solution varies with central substituent and increases according to the following order: Zn(II) complex < Pd(II) and Cu(II) complexes < free base < diacid < Ni(II) complex. This order is consistent with published reports of nonplanar core distortions observed by X-ray crystallography for tetraphenylporphyrin and its metal complexes. The nonplanar conformation characteristic of porphyrin diacids provides an explanation for their atropisomerization rates as well as for spectral shifts observed for the four isomers upon protonation.

Restricted rotation of phenyl rings resulting in the existence of room-temperature stable atropisomers has been demonstrated for a variety of compounds. Early inves-

tigations focused on biphenyls, most notably optically active ortho-substituted biphenyls which undergo thermally induced or photoinduced racemization.¹⁻⁷ More

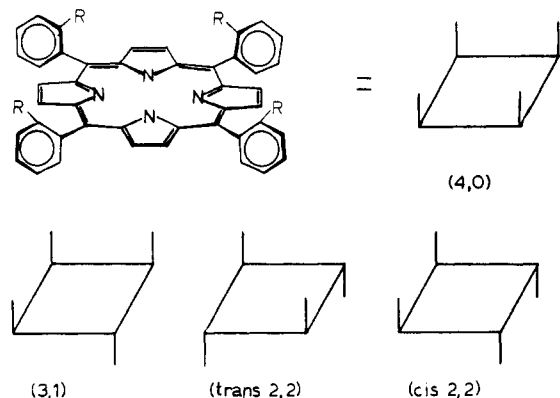


Figure 1. Atropisomers of an ortho-substituted tetraphenylporphyrin. The structure of the (4,0) isomer is given, and all four isomers are represented schematically.

recently, several investigations of the atropisomerism of ortho-substituted tetraphenylporphyrins, their metal complexes, and their dications have been reported.⁸⁻¹³ For such systems, the high-energy barrier associated with the interconversion between atropisomers arises from a steric interaction between the *o*-phenyl substituent and the β -pyrrole hydrogen. As a result of the steric repulsion between these neighboring groups, rotation about the porphyrin-phenyl bond through a coplanar transition state is hindered to such a degree that the ortho substituent is, at room temperature, fixed on one side of the porphyrin plane. The four atropisomers, pictured in Figure 1, correspond to the possible distributions of the four *o*-phenyl substituents between the two sides of the porphyrin plane.

Models show that, when the porphyrin core and phenyl ring are in a coplanar conformation, there is a high degree of contact between the β -pyrrole hydrogen and the *o*-phenyl substituent, and that this unfavorable interaction is maximized when the porphyrin core is in a rigidly planar configuration. In fact, models indicate that substantial deformation from planarity of the porphyrin nucleus is required in order to allow the groups to pass one another in the transition state.⁸ Thus, the rate of atropisomerization is expected to reflect the conformation (i.e., degree of distortion from planarity) and deformability of the porphyrin in solution. X-ray diffraction studies of tetraphenylporphyrin free base,^{14,15} diacid,¹⁶ and numerous

metal complexes¹⁵ have been carried out, and the crystal structures reveal a predominance of nonplanar core configurations. A large degree of variation in the magnitude and symmetry of the core distortion, or "ruffling", is observed as the central substituent is varied. Deviations from planarity observed for the porphyrins in the solid state are at least partially attributable to crystal packing forces,¹⁵ and so it is unlikely that crystal structures accurately reflect the structure of the porphyrin in solution. The atropisomerization process is therefore a useful probe with which to study solution stereochemistry of tetraphenylporphyrin as it depends on the coordinated central substituent, and to compare solution behavior with X-ray structural data.

Several techniques have been used to determine energy barriers of phenyl ring rotation for such systems. Kinetic studies, in which isomerization was monitored with thin layer chromatography and spectrophotometry to separate and determine relative amounts of the four atropisomers, were performed with tetrakis(*o*-hydroxyphenyl)porphyrin and its copper complex.⁸ Free energies of activation of 24 and 25.4 kcal/mol were measured respectively at 23 °C. A value of 26.2 kcal/mol for the rotational barrier of tetrakis(*o*-cyanophenyl)porphyrin at 50 °C was determined by a similar approach.¹³ Dynamic ¹H NMR has been used to estimate the energy barrier to atropisomer interconversion for nickel(II) tetrakis(*o*-tolyl)porphyrinate,⁹ a lower limit of 26 kcal/mol was determined from the separation of the methyl resonances at 180 °C. The free base and diacid of tetrakis(*o*-methoxyphenyl)porphyrin were investigated by use of line shape analysis of ¹H NMR spectra at different temperatures.¹⁰ The average ΔG^\ddagger values for rotation of a single phenyl ring were calculated to be 25.9 and 23.0 kcal/mol, respectively. A similar method has been applied to tetraphenylporphyrin-metal complexes in which the phenyl rings are unsubstituted or para substituted, but one or two different axial ligands are present.¹¹ The ortho hydrogens on the two sides of the porphyrin plane are thus nonequivalent; coalescence of these phenyl resonances has been observed, and rotational barriers calculated for a variety of complexes.¹¹

We previously reported results of an investigation of the atropisomerization of two "picket-fence" porphyrins¹² (tetrakis(*o*-amidophenyl)porphyrins) in which high-performance liquid chromatography proved to be an effective technique for monitoring isomeric ratios. Thermal-induced and photoinduced atropisomerization reactions of tetrakis(*o*-pivalamidophenyl)porphyrin ($H_2PF, TPiv$) and tet-

(1) (a) Turner, E. E.; LeFevre, R. I. W. *Chemistry-Industry* **1926**, 45, 831, 833. (b) Bell, F.; Kenyon, J. *Ibid.* **1926**, 45, 864. (c) Mills, W. H. *Ibid.* **1926**, 45, 884, 905.

(2) Mislow, K.; Gordon, A. I. *J. Am. Chem. Soc.* **1963**, 85, 3521.

(3) Zimmerman, H. E.; Crumrine, D. S. *J. Am. Chem. Soc.* **1972**, 94, 498.

(4) Irie, M.; Yoshida, K.; Hayashi, K. *J. Phys. Chem.* **1977**, 81, 969.

(5) Fischer-Hjalmars, I. *Tetrahedron* **1963**, 19, 1805.

(6) Lewis, G. N.; Kasha, M. *J. Am. Chem. Soc.* **1944**, 66, 2100.

(7) Wagner, P. J. *J. Am. Chem. Soc.* **1967**, 89, 2820.

(8) Gottwald, L. K.; Ullman, E. F. *Tetrahedron Lett.* **1969**, 36, 3071.

(9) Walker, F. A. *Tetrahedron Lett.* **1971**, 52, 4949.

(10) Dirks, J. W.; Underwood, G.; Matheson, J. C.; Gust, D. *J. Org. Chem.* **1979**, 44, 2551.

(11) Eaton, S. S.; Eaton, G. R. *J. Am. Chem. Soc.* **1975**, 97, 3660, and references therein.

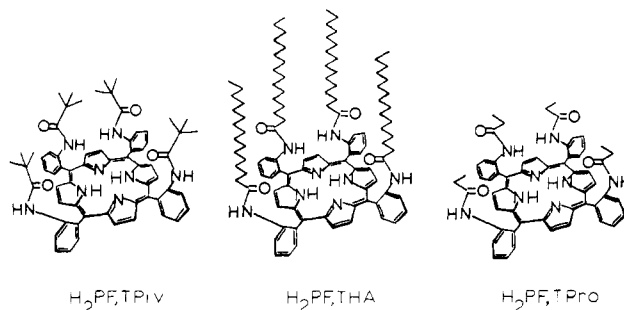
(12) Freitag, R. A.; Mercer-Smith, J. A.; Whitten, D. G. *J. Am. Chem. Soc.* **1981**, 103, 1226.

(13) Hatano, K.; Anzai, K.; Kubo, T.; Tamai, S. *Bull. Chem. Soc. Jpn.* **1981**, 54, 3518.

(14) Hoard, J. L.; Hamor, M. J.; Hamor, T. A. *J. Am. Chem. Soc.* **1963**, 85, 2334.

(15) Fleischer, E. B.; Miller, C. K.; Webb, L. E. *J. Am. Chem. Soc.* **1964**, 86, 2342.

(16) Fleischer, E. B.; Stone, A. L. *J. Am. Chem. Soc.* **1968**, 90, 2735.



rakis(*o*-hexadecanamidophenyl)porphyrin (H_2PF, THA) as well as their copper and zinc complexes were described. This study has been extended to include the shorter chain derivative tetrakis(*o*-propionamidophenyl)porphyrin ($H_2PF, TPro$) and its metal complexes. For the present study, photolytic and thermal atropisomerization processes were monitored for all three picket fence porphyrins, their complexes with divalent Cu, Zn, Ni, and Pd, and their diacids ($H_4PF, TPiv^{2+}$, H_4PF, THA^{2+} , and $H_4PF, TPro^{2+}$).

The relative rates, energy barriers, and quantum yields of atropisomerization are discussed in terms of their implications about the geometry and deformability of the porphyrin core in solution. For the three porphyrin diacids, unusual thermal equilibrium and photostationary state isomeric ratios and reduced rotational barriers were obtained. These have been interpreted in terms of diacid structure based on the results of a spectral comparison of the four isomers in their free base and diacid forms.

Experimental Section

Materials. Benzene (Fisher, Certified ACS Grade) used for photoisomerization reactions was purified by successive washings with concentrated H_2SO_4 , distilled H_2O , dilute NaHCO_3 , and distilled H_2O , followed by distillations over P_2O_5 . Xylenes (Fisher, Certified ACS Grade) were used as received for thermal studies. Solvents for HPLC use, including chloroform, hexanes, ethyl acetate, benzene, and methylene chloride, were obtained from Fisher, Baker, or Mallinckrodt and filtered through Millipore or Rainin filters (0.45- μm pore size).

Palmitoyl chloride (Aldrich), pivaloyl chloride (Baker), and propionyl chloride (Aldrich) were used as received for the preparation of picket-fence porphyrins. Preparation of tetrakis(*o*-aminophenyl)porphyrin ($\text{H}_2\text{PF,TA}$) and isolation of the (4,0) isomer were performed according to previously published methods.¹⁷ Separated isomers of $\text{H}_2\text{PF,TA}$ were obtained from a statistical mixture produced by thermal equilibration using preparative thin layer chromatography (1:1 CHCl_3 :ether) on silica gel.

Preparation of Picket-Fence Porphyrins. (4,0) *Tetrakis(o-pivalamidophenyl)porphyrin* ($\text{H}_2\text{PF,TPiv}$) was prepared by a modification of the procedure described by Collman.¹⁷ (4,0) $\text{H}_2\text{PF,TA}$ was dissolved in methylene chloride. Excess pyridine and pivaloyl chloride were added and the reaction was monitored by TLC (1:1 CHCl_3 :ether) until low R_f spots disappeared (1.5–3 h). The reaction mixture was then stirred with dilute aqueous ammonia, washed with H_2O , and evaporated to dryness. The residue was purified by preparative TLC (1:9 ether: CHCl_3) on 1500- μm silica gel plates.

(4,0) *Tetrakis(o-hexadecanamidophenyl)porphyrin* ($\text{H}_2\text{PF,THA}$) was prepared by addition of excess pyridine and palmitoyl chloride to a solution of (4,0) $\text{H}_2\text{PF,TA}$ in dry distilled benzene. The flask was equipped with a drying tube and the solution was stirred for 1 h. Benzene was removed by rotary evaporation, and the residue dissolved in CHCl_3 . The reaction mixture was then neutralized with dilute aqueous ammonia, washed with H_2O , dried over MgSO_4 , and filtered. The filtrate was concentrated by rotary evaporation and applied to a silica gel column (1 in. \times 12 in.) prepared as a slurry in CHCl_3 . (4,0) $\text{H}_2\text{PF,THA}$ was eluted with 2.5:1 CHCl_3 :ether. Preparative TLC (5% ethyl acetate in CHCl_3) on silica gel was used for purification of small quantities and for isolation of all four isomers from a mixture. *Anal.* Calcd for $\text{C}_{108}\text{H}_{154}\text{N}_8\text{O}_4$: C, 79.66; H, 9.53; N, 6.88. Found for the (4,0) isomer: C, 78.40; H, 9.49; N, 6.43. Found for the (3,1) isomer: C, 79.31; H, 9.52; N, 6.44. UV-visible (benzene): $\epsilon_{423} = 270000$; $\epsilon_{515} = 18800$; $\epsilon_{549} = 5200$; $\epsilon_{590} = 5900$; $\epsilon_{647} = 2100$.

(4,0) *Tetrakis(o-propionamidophenyl)porphyrin* ($\text{H}_2\text{PF,TPro}$) was prepared in analogous fashion to $\text{H}_2\text{PF,THA}$, by the condensation of (4,0) $\text{H}_2\text{PF,TA}$ with propionyl chloride in dry distilled benzene. Following similar workup, $\text{H}_2\text{PF,TPro}$ was purified by preparative

TLC (10% ether in ethyl acetate) on silica gel. UV-visible (benzene): $\epsilon_{422} = 254000$; $\epsilon_{515} = 16600$; $\epsilon_{548} = 4500$; $\epsilon_{589} = 5200$; $\epsilon_{646} = 1800$.

Metallation Reactions. Zn(II) and Cu(II) were inserted into the picket-fence porphyrins by the metal acetate method.¹⁸ NiPF,THA and NiPF,TPro were prepared by combining solutions of nickel acetate in methanol with porphyrin in methylene chloride, and stirring for several hours or overnight. This procedure resulted in atropisomerization; isolation of pure (4,0) Ni(II) complexes was accomplished by HPLC just prior to use. Attempted preparation of NiPF,TPiv by this and other literature methods was unsuccessful. Pd(II) complexes were prepared by heating the porphyrin with bis(benzonitrile)-palladium chloride under reflux in benzene.¹⁹ Unreacted free base porphyrin was removed by cation-exchange chromatography using resin AG 50W-X2 packed as a slurry in HBr/methanol. Pd complexes were eluted with 2% HBr in methanol; dark green protonated porphyrin remained at top of column.

Porphyrin Diacids. Diprotonated picket-fence porphyrins were obtained by the addition of one drop of concentrated HCl to a solution of the porphyrin in benzene immediately prior to photoisomerization. For thermal studies, several drops of concentrated HCl were added to heated xylenes prior to addition of free base porphyrin. Solutions of porphyrin diacids were neutralized by the addition of dilute ammonium hydroxide before analysis of isomeric ratios by HPLC.

Procedures. *Thermal atropisomerization studies* were carried out in stirred xylenes using an oil bath and hot plate to control temperature. The oil bath was heated to the desired temperature and a flask containing 5–10 mL of the xylenes was immersed in it. When the temperature of the xylenes was constant, the (4,0) isomer of porphyrin dissolved in a minimum amount of chloroform was added and the timer started. Aliquots were withdrawn at desired times and placed in an ice bath. The percent isomerization as a function of time was monitored by HPLC. Rate constants and free energies of activation were calculated at the time corresponding to 10% isomerization from (4,0) to (3,1), the initially produced isomer. Thermal equilibrium isomeric ratios were determined by long-term heating until the relative concentrations of the isomers no longer changed.

Photoatropisomerization studies were carried out with a 100-W tungsten source (GE CDS/CDX bulb). A solution of the (4,0) isomer of the porphyrin in dry, distilled benzene was bubble degassed with argon for 15–30 min prior to and during photolysis. Aliquots were withdrawn with a syringe at desired time intervals, and isomerization progress was monitored by HPLC. Photostationary states were determined by irradiating the solutions until the isomeric ratios remained constant. Relative quantum yields for isomerization were determined by using a merry-go-round equipped with a Hanovia 450-W medium-pressure Hg lamp and a Pyrex cooling well. Corning 3-75 and 5-58 filters were used to isolate the 436-nm band. Solutions of (4,0) isomers of the various porphyrins and metalloporphyrins (1×10^{-4} M) in purified benzene were degassed by the freeze-pump-thaw method and sealed at 2×10^{-6} torr prior to irradiation for 2–7 h. Conversion of the (4,0) isomer to the (3,1) isomer was monitored by HPLC.

(18) Furhop, J.; Smith, K. M. In "Porphyrins and Metalloporphyrins"; Smith, K. M., Ed.; Elsevier: Amsterdam, 1975; p 798.

(19) Mercer-Smith, J. A.; Whitten, D. G. *J. Am. Chem. Soc.* **1979**, *101*, 6620.

(17) Collman, J. P.; Gagne, R. R.; Reed, C. A.; Halbert, T. R.; Lang, G.; Robinson, W. T. *J. Am. Chem. Soc.* **1975**, *97*, 1427.

TABLE I: Solvents Used as Mobile Phases for the Separation and Analysis of Atropisomeric Mixtures by HPLC

compd	mobile phase	elution order ^a
H ₂ PF,THA	65% CHCl ₃ -35% hexanes	(4,0); (trans 2,2); (3,1); (cis 2,2)
H ₂ PF,TPiv	20% EtOAc-80% benzene	(trans 2,2); (cis 2,2); (3,1); (4,0)
H ₂ PF,TPro	EtOAc	(trans 2,2); (cis 2,2); (3,1); (4,0)
ZnPF,THA	60% CHCl ₃ -30% hexanes	(4,0); (3,1)
ZnPF,TPiv	15% EtOAc-85% CH ₂ Cl ₂	(3,1); (4,0)
ZnPF,TPro	EtOAc	(3,1); (4,0)
CuPF,THA	65% CHCl ₃ -35% hexanes	(4,0) and (trans 2,2); (3,1); (cis 2,2)
CuPF,TPiv	25% EtOAc-75% benzene	(trans 2,2); (cis 2,2); (3,1); (4,0)
CuPF,TPro	EtOAc	(trans 2,2); (cis 2,2); (3,1); (4,0)
PdPF,THA	7.5% EtOAc-92.5% benzene	(trans 2,2); (4,0); (3,1); (cis 2,2)
PdPF,TPiv	25% EtOAc-75% benzene	(3,1); (4,0)
PdPF,TPro	7.5% THF in EtOAc	(trans 2,2); (cis 2,2); (3,1); (4,0)
NiPF,THA	60% CHCl ₃ -40% hexanes	(4,0); (trans 2,2); (3,1); (cis 2,2)
NiPF,TPro	EtOAc	(trans 2,2); (cis 2,2); (3,1); (4,0)

^a Isomers are listed in order of increasing retention time on a Whatman Partisil 5/25 HPLC column.

High-Pressure Liquid Chromatography. Analytical work was performed with a high-performance liquid chromatography consisting of a Perkin-Elmer Series 1 LC pump and a Varian Vari-Chrom UV-visible detector. A Whatman Partisil 5/25 HPLC column was found to resolve the isomers of most of the compounds studied. Appropriate solvent systems for each of the picket-fence porphyrins and metalloporphyrins are given in Table I along with the elution orders of the atropisomers. In the case of several compounds for which isomerization proceeded slowly, (cis 2,2) and (trans 2,2) isomers were not detected during the time of the isomerization experiment. For these, elution orders of (4,0) and (3,1) isomers only are indicated. Retention times required to obtain sufficient resolution of isomers varied considerably with the *o*-amido group and central substituent. Elution orders were determined in each case by the preparation of each isomer from known samples of the isomers of H₂PF,TA_m, and comparison of retention times to those of the various isomers in a mixture. In some cases atropisomers were identified on the basis of their relative peak areas (a 1:2:4 ratio of (trans 2,2):(cis 2,2):(3,1) is statistically expected). Isomers were detected by optical absorbance at 420 nm (λ_{\max} Soret band). Since the isomers have identical absorption properties,¹² relative concentrations of the four isomers could be determined directly from their relative peak areas in a chromatogram. The flow rate used in all cases was 1 mL/min.

Spectral Studies. Visible spectra were recorded on a Perkin-Elmer 576 UV-visible spectrophotometer. For the diacid spectral comparisons, picket-fence porphyrin isomers were prepared from the appropriate isomers of H₂PF,TA_m (in analogous fashion to the preparation of (4,0) isomers). Free base porphyrin was dissolved in benzene and the spectrum was recorded from 450 to 700 nm. The porphyrin was then protonated by the addition of one drop concentrated HCl, and the spectrum of the resulting green solution was recorded.

TABLE II: Isomeric Mixtures Produced by Thermal Equilibration of Picket-Fence Porphyrin

porphyrin	thermal equilibrium			
	% (4,0)	% (3,1)	% (trans 2,2)	% (cis 2,2)
statistical	12.5	50	12.5	25
H ₂ PF,THA	4	47	20	29
CuPF,THA	2	48	20	30
NiPF,THA	4	46	18	32
PdPF,THA	2	50	18	30
H ₄ PF,THA ²⁺	3	37	33	27
H ₂ PF,TPro	11	52	15	22

Results and Discussion

Thermal Atropisomerization. For all of the porphyrins studied, thermal interconversion between atropisomers was found to occur by rotation about a single porphine-phenyl bond. The (4,0), (trans 2,2), and (cis 2,2) isomers can thus interconvert directly through the (3,1) isomer only. Isomerization of (3,1), however, depending on which of its three nonequivalent phenyl rings undergoes rotation, can lead to any of the other three atropisomers. Heating of the (4,0) isomer of a picket-fence porphyrin results in initial production of (3,1). Following substantial buildup (10–20%) of the (3,1) isomer, (trans 2,2) and (cis 2,2) appear in roughly a 1:2 ratio. Eventually a thermal equilibrium mixture is reached.

Equilibrium isomeric ratios are shown in Table II for a variety of picket-fence porphyrins and metalloporphyrins. For H₂PF,THA and its Cu, Ni, and Pd complexes, the equilibrium mixtures observed are identical within experimental error. The distribution of isomers for these compounds varies significantly from the statistical distribution only for the (4,0) and (trans 2,2) isomers. This apparently results from an unfavorable interaction between adjacent long-chain ortho substituents on the same side of the porphyrin plane. Thus, a smaller amount of the (4,0) isomer, for which there are four such interactions, and a larger amount of the (trans 2,2) isomer, for which such steric interactions are eliminated, are present at equilibrium. For the free base and metal complexes, there appears to be no effect of central substituent on equilibrium ratio. The Zn complex was seen to undergo decomposition at the long times and high temperatures required; equilibration between isomers was therefore not observed. A very slight deviation from the statistical distribution of isomers is observed for H₂PF,TPro at equilibrium. For this shorter chain derivative, the interaction between adjacent ortho substituents is less significant; the magnitude of the difference between observed and expected ratios is smaller than with H₂PF,THA. The unusual equilibrium mixture observed for the diacid H₄PF,THF²⁺ is discussed in a later section.

Atropisomerization rates for the three free base picket-fence porphyrins were measured as a function of temperature. The rate constants and activation parameters are given in Table III. By comparing the free energies of activation at any temperature, it is evident that H₂PF,TPro and H₂PF,THA have equal energy barriers to rotation in spite of their differing chain lengths. This indicates that the steric interaction responsible for the hindered rotation occurs at the amido group and the first few carbons of the attached chain. Interaction between the hexadecyl group and the rest of the porphyrin molecule upon phenyl ring rotation apparently does not significantly increase the activation barrier. The presence of the bulky *tert*-butyl group of H₂PF,TPiv, on the other hand, increases the ΔG^\ddagger by an average of 1.6 kcal/mol at any

TABLE III: Rate Constants and Activation Parameters for the Atropisomerization (4,0 → 3,1) of Picket-Fence Porphyrins as a Function of Temperature

H ₂ PF, TPro			H ₂ PF, THA			H ₂ PF, TPiv		
T, °C	k, s ⁻¹	ΔG [‡] , kcal/mol	T, °C	k, s ⁻¹	ΔG [‡] , kcal/mol	T, °C	k, s ⁻¹	ΔG [‡] , kcal/mol
76	5.6 × 10 ⁻⁶	28.9	79	7.8 × 10 ⁻⁶	28.9			
96	4.4 × 10 ⁻⁵	29.1	99	6.9 × 10 ⁻⁵	29.0	96	6.7 × 10 ⁻⁶	30.5
112	2.4 × 10 ⁻⁴	29.1	114	3.3 × 10 ⁻⁴	29.0	111	3.1 × 10 ⁻⁵	30.6
127	1.0 × 10 ⁻³	29.1	125	8.7 × 10 ⁻⁴	29.1	123	9.4 × 10 ⁻⁵	30.7
135	1.9 × 10 ⁻³	29.2	133	1.8 × 10 ⁻³	29.1	133	2.0 × 10 ⁻⁴	30.9
	ΔH [‡] = 27.5			ΔH [‡] = 27.5			ΔH [‡] = 26.7	
	ΔS [‡] = -4			ΔS [‡] = -4			ΔS [‡] = -10	

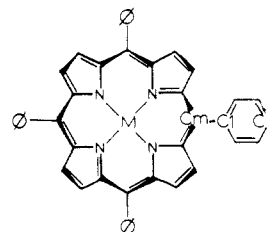
TABLE IV: Free Energy of Activation for the Atropisomerization of Picket-Fence Porphyrins as a Function of Central Substituent

M	ΔG [‡] , kcal/mol		
	MPF, TPro	MPF, THA	MPF, TPiv
free base (H ₂)	29.1	29.1	30.6
diacid (H ₄)	26.4	26.5	28.3
Ni(II)	25.8	25.8	
Cu(II)	29.7	29.6	31.4
Pd(II)	31.0	31.1	31.7
Zn(II)	31.4	31.2	32.2

temperature. The temperature effect is similar for all three picket-fence porphyrins. A small negative entropy of activation and a large enthalpy of activation are associated with the rotation process. The negative entropies observed over a large number of temperatures are somewhat smaller than those obtained in previous studies using few temperatures;^{12,13} the reason for this is not apparent.

So that the effect of the central substituent on the rotational energy barrier could be determined, thermal atropisomerization reactions of the picket-fence porphyrin metal complexes and diacids were studied at one temperature (110 ± 3 °C). The results are given in Table IV. As was observed with the free base porphyrins, the complexes of H₂PF, TPiv exhibit slower isomerization than the corresponding H₂PF, TPro and H₂PF, THA complexes. With each central substituent, the two straight-chain porphyrins have equal rotational energy barriers. It is obvious from the results in Table IV that the ease of isomerization (i.e., the ease of rotation about the porphine-phenyl bond) is affected by the atom(s) coordinated to the porphine core. The dependence of the rotational energy barrier on the central substituent is found to be the same for all three porphyrins studied. The Ni complexes and diacids are seen, in all cases, to have lower activation barriers than the free base porphyrins, while the Pd and Cu complexes isomerize less readily. The slowest isomerization rates are found for the Zn complexes; restricted rotation resulting from complexation with Zn accounts for an increase in ΔG[‡] of about 2 kcal/mol.

The rate of atropisomerization of an ortho-substituted tetraphenylporphyrin is expected to reflect the ability of the porphyrin core to undergo nonplanar deformation. Ruffling of the porphine core increases the distance between the ortho substituent and the pyrrole hydrogen, thereby reducing the interaction responsible for restricted phenyl ring rotation. This is consistent with the observation that, in the solid state, there exists a correlation between planarity of the porphine core and perpendicularity (with respect to the mean porphyrin plane) of the phenyl ring.^{8,10,11} The variation in atropisomerization rate as the central substituent is changed suggests that in solution the degree of nonplanarity that can be achieved by the porphyrin nucleus varies according to the steric requirements of the coordinated atom(s).

Figure 2. D_{2d} ruffled conformation exhibited by H₂TPP and its metal complexes (see ref 8). Magnitudes of the out-of-plane displacements indicated here are given in Table V.TABLE V: Summary of Structural Data Obtained by X-ray Crystallography for H₂TPP and Its Metal Complexes Showing the Effect of Shortened M-N Bonds on the Degree of Distortion from Planarity

porphyrin	M-N distance, Å	displacement from mean plane, ^a Å			ref
		Cm	C1	C2	
H ₂ TPP		±0.38	±0.73	±1.43	7
NiTPP	1.928	±0.51 (for NiOEP)			8, 15
PdTPP	2.009	±0.38	±0.75	±1.44	8
CuTPP	1.981	±0.42	±0.75	±1.42	8
ZnTPP	2.036	0	0	0	8

^a Cm, C1, and C2 are labeled on Figure 2.

As evidenced by crystal structure data, steric requirements of coordinated metal atoms result in deviations from the optimum porphyrin center to nitrogen distance, estimated to be 2.01 Å.²⁰ Although the porphyrin ligand is unable to expand or contract radially, Hoard²¹ has shown that deformation normal to the porphyrin plane can effectively shorten M-N distances without altering other bond lengths or angles, thus relieving the strain resulting from core contraction. For an expanded core, on the other hand, nonplanar distortions cannot relieve the angular strain and are therefore less likely to occur. Displacement of the metal atom away from the center of the rigidly planar porphyrin allows for longer M-N bonds. Crystal structures of tetraphenylporphyrin (H₂TPP) and its Ni, Cu, and Pd complexes reveal that, with each of these central substituents, the porphyrin exhibits a D_{2d} ruffled conformation in which the methine carbons are alternately displaced above and below the porphyrin plane¹⁵ (Figure 2). The magnitude of the deformation correlates with the extent to which the M-N bond lengths are shortened, as shown in Table V. Although a quantitative NiTPP structure has not been published, it is expected, based on its extreme M-N shortening and the large methine carbon displacement reported for nickel octaethylporphyrinate (NiOEP),²² to exist in the most ruffled conformation. A

(20) Collins, D. M.; Hoard, J. L. *J. Am. Chem. Soc.* 1970, 92, 3761.

(21) Hoard, J. L. *Ann. N.Y. Acad. Sci.* 1973, 206, 18.

(22) Meyer, E. F.; Jr. *Acta Crystallogr., Sect. B* 1972, 28, 2162.

planar configuration of the porphine nucleus is confirmed by X-ray crystallography for ZnTPP,¹⁵ in which the coordinated Zn ion requires relatively long M-N bonds.

The relative ΔG^* values for phenyl ring rotation obtained with the picket-fence derivatives of TPP are quite consistent with the evidence for porphyrin deformability provided by the crystal structures. The nickel complex, which in the solid state has the most nonplanar conformation, exhibits the most facile isomerization. The fact that the Ni complexes undergo isomerization more readily than the free base porphyrins indicates that the solution conformation of the Ni porphyrins is, on the average, more deformed from planarity than that of the uncomplexed porphyrins. The free base, Pd, and Cu complexes of TPP exhibit similar degrees of ruffling in their crystalline forms. The Cu complex has a more contracted core than the Pd complex, and, with the picket-fence derivatives, the rotational energy barrier was found to be somewhat lower with Cu as the central substituent than with Pd. In the absence of a coordinated metal, however, the atropisomerization becomes more facile. This is not surprising since, although the magnitudes of the "allowed" deformations are similar to those of the Cu and Pd complexes, one would expect the unconstrained free base porphyrin to more readily undergo the nonplanar deformation than the coordination complexes. Gottwald and Ullman⁸ also noted an increase in ΔG^* for the isomerization of tetrakis(*o*-hydroxyphenyl)porphyrin on going from the free base to the Cu complex. The energy barrier difference was attributed to the formation of a hydrated five-coordinate Cu porphyrin, which would be expected to be more rigid. The present study shows that the energy barrier increases for Cu complexes in the absence of water and for Pd complexes for which five-coordinate species would not be formed. The zinc complexes have extremely high rotational barriers, consistent with the planar configuration observed by crystallography of ZnTPP. It is apparent that in solution, as in the solid state, the Zn porphyrin is planar and much more rigid than the free base and other metalloporphyrins studied. A discussion of the low-energy barriers observed for the picket-fence porphyrin diacids is saved for a later section.

These results, although they do not require that porphyrins achieve the same structure in solution as in the solid state, do suggest a correlation between solution conformation and deformability, and the degree of distortion seen in the crystal structures. The solid-state conformation may represent a "limit of deformability" of the porphyrin molecule, which, in solution, may be flipping rapidly between planar and nonplanar forms. Coordination of a metal atom to the porphine core can have the effect of either stabilizing a planar conformation (thereby lowering the isomerization rate) or a nonplanar conformation (thereby increasing the rate).

Photoatropisomerization. Photochemical interconversion between atropisomers has been previously reported for several substituted biphenyl derivatives.³⁻⁵ Racemization of these compounds proceeds via an excited state which is characterized by an enhanced intraannular bond order over that of the ground state. The barrier to rotation of the phenyl rings through a coplanar transition state is therefore reduced in the excited state.

Atropisomerization of picket-fence porphyrins can also be accomplished photochemically at room temperature. Whether this photoprocess originates from electronic properties of the excited state (i.e., resonance stabilization of coplanar transition states as proposed for the biphenyls) or changes in steric properties upon excitation (i.e., sta-

TABLE VI: Photostationary States and Quantum Yields (ϕ) for the Photoatropisomerization of Picket-Fence Porphyrins

compd	photostationary state				$\phi_{4,0 \rightarrow 3,1}$
	% (4,0)	% (3,1)	% (trans 2,2)	% (cis 2,2)	
H ₂ PF,THA	5	48	20	27	1.3×10^{-3}
H ₂ PF,THA ²⁺	6	13	80	1	1.7×10^{-3}
PdPF,THA	7	56	13	24	7.1×10^{-4}
ZnPF,THA	7	49	18	26	1.9×10^{-4}
H ₂ PF,TPro	9	50	16	25	2.3×10^{-3}
H ₂ PF,TPro ²⁺	0	22	78	0	

bilization of a ruffled configuration or an increase in the deformability of the porphyrin core) is unclear. For the picket-fence porphyrins, the situation is made more complex by the presence of four sites at which atropisomerization can take place. A variety of interconversion pathways, ranging from a "one-bond activation" process to a "total randomization" process (in which all four phenyl ring experience reduced rotational barriers), can be visualized. However, due to the low quantum yields associated with photoatropisomerization (Table VI), these possible mechanisms are essentially indistinguishable. The fraction of absorbed photons resulting in an atropisomerization event is low; the probability of two such events occurring simultaneously is negligible. Therefore, although in most cases initial product studies indicate that interconversion proceeds by rotation of a single phenyl ring, this does not rule out the existence of an excited state in which more than one phenyl ring experiences an increased tendency for coplanarity. There is some evidence that the photoisomerization of H₂PF,THA proceeds via a mechanism in which opposite phenyl rings can rotate simultaneously.¹² However, this was not observed with the other two free base picket fence porphyrins.

The excited state leading to the photointerconversion of atropisomers was confirmed by oxygen quenching studies to be a triplet state. The isomerization process was completely quenched in the presence of oxygen, even at concentrations at which negligible fluorescence quenching was observed. Under deoxygenated conditions, photoatropisomerization occurred for the free base picket-fence porphyrins, their diacids, and their Pd and Zn complexes. The Ni and Cu porphyrins, which typically are characterized by extremely short triplet lifetimes, do not undergo photoisomerization. Photostationary state isomeric ratios, given in Table VI, agree quite closely in most cases with the ratios observed at thermal equilibrium. Again, for the free base and metallo complexes, the agreement with the statistical distribution is good with the exception of the enhanced amount of (trans 2,2) and diminished amount of (4,0) isomers. The deviations from the statistical ratio are greater for the H₂PF,THA complexes than for the shorter chain H₂PF,TPro complexes, as was found with the thermal equilibrium mixtures. Photostationary states for the three picket-fence porphyrin diacids are very different from those observed for the free base and metalloporphyrins. The extreme enrichment of the (trans 2,2) isomer implies that the isomeric distribution is not controlled by statistics, but rather by the relative energies of the isomers. An explanation for this is offered in the next section.

The quantum yields for the conversion of (4,0) to (3,1) were measured for the long-chain picket-fence porphyrin free base, diacid, and metal complexes for which photoisomerization occurred (Table VI). It is clear from these results that the excited-state atropisomerization process

is subject to the same deformability requirements that governed the ground state (thermal) atropisomerization rates. The lowest quantum yield for rotation of a single phenyl ring is observed for the planar Zn complex. Isomerization of the free base porphyrin is more efficient than that of the Pd or Zn complex. A slight increase in the quantum yield on going from the free base to the diacid form is also noted. Based on the relative energy barriers of the ground-state rotation process for these two species, one would expect a greater difference in the two quantum yields. However, the excited triplet state lifetime of the diacid species (70 μ s) is more than 15 times shorter than that of the free base (1100 μ s). The fact that the quantum yields are similar implies that the ease of rotation of a phenyl ring in the excited state is greatly enhanced for the diacid over that of the free base. The quantum yield for the atropisomerization of $H_2PF,TPro$ was also measured relative to that of H_2PF,THA . Interestingly, the photoisomerization of the short-chain porphyrin is almost twice as efficient as that of the long-chain porphyrin is almost twice as efficient as that of the long-chain derivative, although the two have identical ground state (thermal) isomerization rates. Thus, of the two processes, the photoinduced atropisomerization is more sensitive to ortho substituent chain length.

Porphyrin Diacids. Acidification of a porphyrin molecule yields a dicationic species in which all four pyrrole nitrogens are protonated. The steric repulsion resulting from the presence of four inner-core hydrogen atoms causes the pyrrole rings to tilt alternately up and down with respect to the mean porphyrin plane. An X-ray structural determination of the tetraphenylporphyrin diacid, $(H_4TPP)Cl_2$,¹⁶ reveals the angle of this tilt to be 28°. This corresponds to a displacement of the β -pyrrole carbons from the porphyrin plane of close to 0.9 Å. Thus, the steric interaction between the *o*-phenyl and β -pyrrole hydrogen atoms is greatly reduced, and the phenyl rings are able to achieve a more coplanar conformation in which the dihedral angle is reduced to 21°.

Picket-fence porphyrin diacids are expected to have the same core conformation as that of the unsubstituted tetraphenylporphyrin diacid. The presence of the ortho substituents should increase the angle between the phenyl rings and the porphyrin plane over that observed for $(H_4TPP)Cl_2$. However, this angle, as well as the energy barrier associated with rotation of the phenyl ring through coplanarity, is expected to be lowered relative to the free base picket-fence porphyrins. Thus, on the basis of the extreme core distortion, it is not surprising that the atropisomerization proceeds more readily for the porphyrins in their diprotonated forms. For $(H_4PF,TPro)Cl_2$, $(H_4PF,THA)Cl_2$, and $(H_4PF,TPiv)Cl_2$, the free energies of activation are decreased relative to the corresponding free base porphyrins by 2.7, 2.6, and 2.3 kcal/mol, respectively. A decrease in ΔG^\ddagger for phenyl ring rotation of 2.9 kcal/mol was observed by Gust and co-workers¹⁰ on going from the free base to the diacid of tetrakis(*o*-methoxyphenyl)porphyrin. The reduced steric interaction resulting from pyrrole ring tilting is also most likely responsible for the increased quantum yield for atropisomerization, in spite of the shortened lifetimes, observed for $(H_4PF,THA)Cl_2$.

Changes in the visible absorption properties of the macrocycle occur upon protonation of the core.²³ The increase in symmetry results in degeneracy of the two sets of visible bands, and so the third and fourth bands disappear. The nonplanar deformation of the porphyrin core

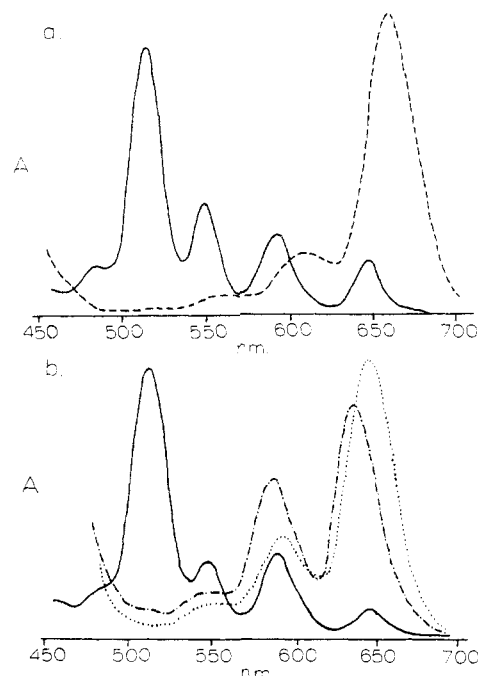


Figure 3. Visible absorption spectra of porphyrins and their diacids recorded in benzene: (a) —, H_2TPP ; ---, $(H_4TPP)Cl_2$; - · - ·, $((4,0)H_4PF,TPiv)Cl_2$; · · · ·, $((trans\ 2,2)H_4PF,TPiv)Cl_2$.

TABLE VII: Comparison of Spectral Shifts Observed upon Protonation for H_2TPP and the Four Atropisomers of Each Picket-Fence Porphyrin^a

porphyrin	λ_{max} band I, nm		λ_{max} band II, nm		total shift, nm
	free base	diacid	free base	diacid	
H_2TPP	648	661	592	609	+30
H_2PF,THA					
(4,0)	647	643	591	592	-3
(trans 2,2)	648	654	591	600	+15
(3,1)	647	651	591	598	+11
(cis 2,2)	648	649	591	597	+7
$H_2PF,TPiv$					
(4,0)	647	638	590	589	-10
(trans 2,2)	648	651	591	598	+10
(3,1)	646	646	591	594	+3
(cis 2,2)	646	647	590	593	+4
$H_2PF,TPro$					
(4,0)	647	644	591	592	-2
(trans 2,2)	647	656	590	603	+22
(3,1)	647	650	590	597	+10
(cis 2,2)	647	650	590	598	+11

^a All spectra were recorded in benzene.

disrupts the π -system and results in loss of conjugation. This is seen as a blue shift of the first and second visible bands for the diacids of octaalkylporphyrins.²³ However, for the tetraphenylporphyrin diacid, the increase in conjugation resulting from interaction of the almost coplanar phenyl π -systems with the porphyrin π -system results in a red shift of the visible bands.¹⁶ Spectra of H_2TPP and $(H_4TPP)Cl_2$ are shown in Figure 3a. Thus, from the direction and magnitude of the spectral shifts observed upon protonation, one can infer structural information about the diacids. In particular, the relative degrees of coplanarity achieved by the phenyl rings for a series of diacids can be compared.

Such a study was carried out for the various isomers of the picket-fence porphyrins. Although the atropisomers of the free base porphyrins exhibit identical absorption properties, the position and relative intensities of the two diacid absorption bands vary substantially for different

(23) Gouterman, M. In "The Porphyrins"; Dolphin, D., Ed.; Academic Press: New York, 1978; Vol. 3, p 17.

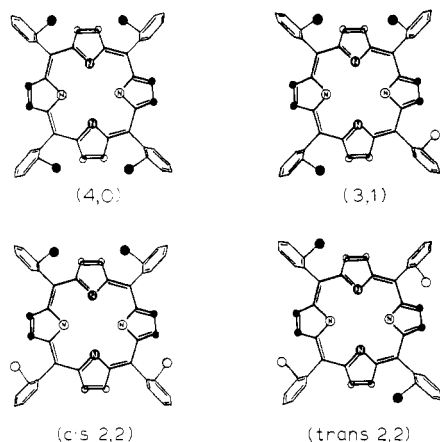


Figure 4. Representations of the four atropisomers of the picket-fence porphyrin diacids showing core conformation and direction of phenyl ring tilting: ●, above the mean plane of the porphyrin; ○, below the mean plane of the porphyrin.

isomers of the same porphyrin. As shown in Figure 3b, the (4,0) isomer of $H_2PF,TPiv$ exhibits a blue shift upon protonation, while the diacid of the (trans 2,2) isomer is significantly red shifted. The λ_{max} values for the first and second visible bands of the free base porphyrins and diacids are compared in Table VII, with the total shift upon protonation indicated in the last column. The higher energy transitions observed for each isomer of $H_4PF,TPiv^{2+}$ relative to those of H_4PF,THA^{2+} and $H_4PF,TPro^{2+}$ are consistent with the idea that the positions of the absorption bands reflect the relative degrees of tilting of the phenyl rings toward the porphyrin plane. With the bulky *tert*-butylamido group the phenyl rings should be constrained to a more perpendicular orientation than with the straight chain ortho substituents, and thus larger blue shifts (and smaller red shifts) are observed. In each case, the diacid spectrum of the (4,0) isomer is blue shifted, while that of the (trans 2,2) isomer is red shifted relative to the free base spectrum. Intermediate spectral shifts are seen for the (cis 2,2) and (3,1) isomers. This implies that the interactions of the phenyl and porphyrin π -systems in the diacids increase in the order (4,0) < (3,1) and (cis 2,2) < (trans 2,2).

The differences in the abilities of the phenyl rings of the various isomers to participate in conjugation with the macrocycle can be explained on the basis of the nonplanar distorted conformation of the diprotonated porphyrin core. The β -pyrrole carbons and hydrogens, with which the *o*-phenyl substituent interacts, are displaced in alternate directions normal to the porphyrin plane. A phenyl ring, in order to rotate from a perpendicular orientation, must tilt such that its ortho substituent points toward the pyrrole carbons which are displaced toward the opposite side of the porphyrin plane (see Figure 4). Thus the phenyl rings of the (4,0) isomer, in which all four substituents are above the porphyrin plane (solid circles), will tilt toward the pyrrole rings whose β -carbons and hydrogens are beneath the porphyrin plane (open circles). This results in tilting of adjacent ortho substituents toward each other, producing unfavorable steric interactions. For the (4,0) isomer, therefore, substantial rotation of the phenyl rings toward coplanarity is prevented, and a minimum of interaction with the porphyrin π -system is allowed. A similar analysis for the (3,1) and (cis 2,2) isomers reveals that, for each of these isomers, two adjacent phenyl rings encounter a steric repulsion between their ortho substituents. The other two phenyl rings are able to achieve a more coplanar orientation, which accounts for the slight red shift observed in the spectra of these two isomers. For

the (trans 2,2) isomer, there are no adjacent ortho substituents on the same side of the porphyrin plane. Each of the four phenyl rings is able to tilt in an appropriate direction to avoid interactions with the pyrrole rings as well as between ortho groups. Although the degree of coplanarity achieved by the phenyl rings of a (trans 2,2) picket-fence porphyrin diacid is less than that achieved by the phenyl rings of H_4TTP^{2+} , the resulting spectral shift is substantial.

The enhanced preference for the (trans 2,2) isomer in both the thermally equilibrated mixture and the photostationary state of the diacids can now be understood. It is clear from the diagrams shown in Figure 4 as well as from the relative red shifts of the visible bands that (trans 2,2) is the lowest energy isomer. The minimization of unfavorable steric interactions and the increased conjugation possible for the diacid (trans 2,2) isomer make it more energetically favored than the other three atropisomers of the porphyrin diacids. The isomeric mixture produced by thermal equilibration of H_4PF,THA^{2+} contains more than twice the expected amount of the (trans 2,2) isomer. In the excited state, the energy difference between the (trans 2,2) isomer and the other three isomers is even greater. The (trans 2,2) isomer accounts for 80% of the total in the photostationary state. This is consistent with the lower energy transitions observed spectrophotochemically for the (trans 2,2) isomer of the diacids.

Conclusion

The results of this study indicate that the atropisomerization reaction is indeed a useful probe of porphyrin solution properties. The effect of central substituent on porphyrin geometry and deformability can be evaluated by monitoring the atropisomerization process. A correlation between nonplanar core distortions seen in crystal structures and both thermal atropisomerization rates and photoatropisomerization efficiencies has been demonstrated.

Acknowledgment. We are grateful to the National Institutes of Health (Grant No. 15238-12) and the U.S. Army Research Office (Grant No. DAAG29-80-K-0066) for support of this work.

Registry No. (4,0)- $H_2PF,TPro$, 86727-60-8; (4,0)- $H_2PF,TPro-2HCl$, 86782-63-0; (4,0)- $NiPF,TPro$, 86727-61-9; (4,0)- $CuPF,TPro$, 86727-62-0; (4,0)- $PdPF,TPro$, 86727-63-1; (4,0)- $ZnPF,TPro$, 86727-64-2; (4,0)- H_2PF,THA , 68561-00-2; (4,0)- $H_2PF,THA-2HCl$, 86782-64-1; (4,0)- $NiPF,THA$, 86727-65-3; (4,0)- $CuPF,THA$, 77057-99-9; (4,0)- $PdPF,THA$, 86727-66-4; (4,0)- $ZnPF,THA$, 77001-07-1; (4,0)- $H_2PF,TPiv$, 55253-62-8; (4,0)- $H_2PF,TPiv-2HCl$, 86782-65-2; (4,0)- $CuPF,TPiv$, 86727-67-5; (4,0)- $PdPF,TPiv$, 86727-68-6; (4,0)- $ZnPF,TPiv$, 86782-69-6; (trans 2,2)- H_2PF,THA , 77027-54-4; (3,1)- H_2PF,THA , 77027-23-7; (cis 2,2)- H_2PF,THA , 77027-24-8; (trans 2,2)- $H_2PF,TPiv$, 77027-26-0; (cis 2,2)- $H_2PF,TPiv$, 77027-27-1; (3,1)- $H_2PF,TPiv$, 77027-25-9; (trans 2,2)- $H_2PF,TPro$, 86782-66-3; (cis 2,2)- $H_2PF,TPro$, 86782-67-4; (3,1)- $H_2PF,TPro$, 86782-68-5; (3,1)- $ZnPF,THA$, 77057-96-6; (3,1)- $ZnPF,TPiv$, 86782-70-9; (3,1)- $CuPF,THA$, 77000-96-5; (trans 2,2)- $CuPF,THA$, 77057-94-4; (3,1)- $CuPF,THA$, 77000-96-5; (cis 2,2)- $CuPF,THA$, 77057-95-5; (trans 2,2)- $CuPF,TPiv$, 86782-72-1; (cis 2,2)- $CuPF,TPiv$, 86727-69-7; (3,1)- $CuPF,TPiv$, 86782-73-2; (trans 2,2)- $CuPF,TPro$, 86782-74-3; (cis 2,2)- $CuPF,TPro$, 86782-75-4; (3,1)- $CuPF,TPro$, 86782-76-5; (trans 2,2)- $PdPF,THA$, 86782-77-6; (3,1)- $PdPF,THA$, 86782-78-7; (cis 2,2)- $PdPF,THA$, 86782-79-8; (3,1)- $PdPF,TPiv$, 86782-80-1; (trans 2,2)- $PdPF,TPro$, 86782-81-2; (cis 2,2)- $PdPF,TPro$, 86782-82-3; (3,1)- $PdPF,TPro$, 86782-83-4; (trans 2,2)- $NiPF,THA$, 86782-84-5; (3,1)- $NiPF,THA$, 86782-85-6; (cis 2,2)- $NiPF,THA$, 86782-86-7; (trans 2,2)- $NiPF,TPro$, 86782-87-8; (cis 2,2)- $NiPF,TPro$, 86782-88-9; (3,1)- $NiPF,TPro$, 86782-89-0; (4,0)- H_2PF,TAm , 68070-27-9; pivaloyl chloride, 3282-30-2; palmitoyl chloride, 112-67-4; propionyl chloride, 79-03-8.